

Double- CO_3^{2-} Centered $[\text{Co}^{\text{II}}_5]$ Wheel and Modeling of Its Magnetic Properties

Mrinal Sarkar,^[a] Guillem Aromí,^{*,[b]} Joan Cano,^{*,[c, d]} Valerio Bertolasi,^[e] and Debashis Ray^{*,[a]}

Abstract: A high-spin Co^{II} cluster with a rare pentagonal molecular structure and formula $[\text{Co}_5(\text{CO}_3)_2(\text{bpp})_5]\text{ClO}_4$ (**1**; Hbpp is 2,6-bis(phenyliminomethyl)-4-methylphenolate) has been synthesized and characterized by single-crystal X-ray diffraction. This topology arises from *fusing* five $[\text{Co}_2(\text{bpp})]$ moieties in a cyclic manner around two CO_3^{2-} central ligands, resulting in propeller-like configuration. The irregular coordination of the carbonate ions to the metal centers results in a combination of co-

ordination numbers (CNs) of the Co^{II} ions of five and six. The bulk magnetization of this complicated magnetically exchanged system has been modeled successfully by employing a matrix diagonalization technique. For this, the

Keywords: carbonate ligands • carbonates • cobalt • coordination chemistry • density functional calculations • magnetic properties • spin-orbit coupling

combination of $S=3/2$ ions (CN=5) with ions exhibiting strong spin-orbit coupling (CN=6) has been considered and a perturbative approach to handle the data in the whole studied range of temperatures (2–300 K) yielding parameters of g and D (for the five-coordinate Co^{II} ions), of A , κ , λ , and Δ (for the metals with spin-orbit coupling) and of the exchange constants J . The agreement with results from DFT calculations, also presented here, is remarkable.

Introduction

The self-assembly of transition-metal macrocycles and molecular spin clusters has become a frontier topic of contemporary research in synthetic coordination chemistry. Apart from having aesthetically pleasing architectures (e.g. squares,^[1] rectangles,^[2] or pentagons^[3]) polymetallic clusters display unique magnetic properties at the molecular level such as single-molecule magnet (SMM) behavior,^[4,5] quantum tunneling of the magnetization,^[6] or quantum interference.^[7] Most of the reported SMMs of 3d ions are based on the metals Mn, Ni, and Fe.^[5] The proliferation of new examples and the investigation of their physical properties have generally been accompanied by the development of the appropriate models to describe their magnetic and spectroscopic behavior, and this process has taken place synergistically, bringing the state of the art of molecular nanomagnetism to the current level. The case of six-coordinate cobalt(II) is special; large single ion anisotropy caused by a first-order orbital contribution to the magnetic moment makes this ion a good candidate to make SMMs^[8] and single-chain magnets (SCMs),^[9] but it also strongly hampers the description of its magnetic behavior, which slows down progress in this direction. Attempts to address this problem have been made for quite a long time. Originally, only perfectly octahe-


[a] Dr. M. Sarkar, Prof. D. Ray
Department of Chemistry, Indian Institute of Technology
Kharagpur 721 302 (India)
Fax: (91) 3222-82252
E-mail: dray@chem.iitkgp.ernet.in

[b] Dr. G. Aromí
Departament de Química Inorgànica, Facultat de Química
Universitat de Barcelona
Diagonal, 647, 08028-Barcelona (Spain)
E-mail: guillem.aromi@qi.ub.es

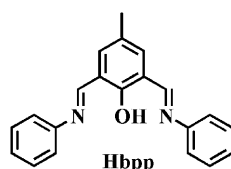
[c] Dr. J. Cano
Institut de Ciència Molecular (ICMol) and Fundació General de la
Universitat de València (FGUV), Universitat de València
46980 Paterna, València (Spain)
E-mail: joan.cano@qi.ub.es

[d] Dr. J. Cano
Institució Catalana de Recerca i Estudis Avançats (ICREA)
Passeig Lluís Companys 23, 08010 Barcelona (Spain)

[e] Prof. V. Bertolasi
Dipartimento di Chimica e Centro di Strutturistica Diffraattometrica
Università di Ferrara
Via Borsari 46, 44100 Ferrara (Italy)

 Supporting information (synthesis of Hbpp, details on UV/Vis and IR spectroscopy) for this article is available on the WWW under <http://dx.doi.org/10.1002/chem.201001418>.

dral systems were considered,^[10] which precluded the inclusion of magnetic anisotropy. The latter has been taken into account in recent models making use of various diagonalization techniques or even providing approximate analytical expressions of the paramagnetic susceptibility for dinuclear Co^{II} complexes.^[11–13] More recently, some of us have proposed a convenient model to treat the magnetic exchange within polynuclear clusters of axially distorted six-coordinate cobalt(II) ions invoking a perturbational approach, which greatly reduces the size of the matrices to be diagonalized.^[14] We report here the synthesis and structure of a rare [Co^{II}₅] wheel, assembled by the bridging action of the Schiff-base ligand Hbpp (2,6-bis(phenyliminomethyl)-4-methylphenol, Scheme 1)^[15] and the template effect of two carbonate ions, with the formula [Co₅(CO₃)₂(bpp)₅]ClO₄ (**1**). The

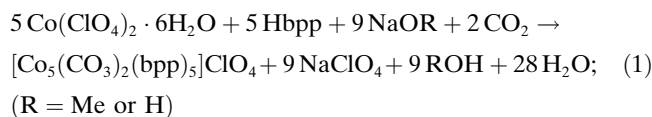


Scheme 1. Structure of Hbpp.

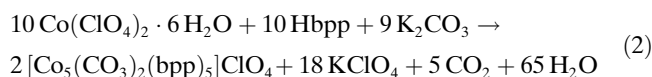
ligand Hbpp should favor the assembly of dinuclear moieties with vacant coordination sites, which should therefore be prone to bind to other exogenous donors, eventually facilitating the growth of the system into higher nuclearity species. Surprisingly, only mononuclear complexes have been reported with this ligand or close derivatives,^[16,17] even though this principle has been proven with related Schiff bases in the construction of large clusters.^[18] This potential is exploited here, together with the capacity of the carbonate ligand to adopt a large variety of coordination modes,^[19–24] to access the rare topology featured by complex **1**. The singularity of the bridging motifs present in this cluster makes it for an interesting species to study its intramolecular magnetic exchange. These interactions are described here theoretically, following a study by DFT calculations. Most remarkably, a good simulation of the experimental bulk magnetization data is provided by using the above-mentioned model, where both types of metal centers found in **1** have been considered; high-spin five-coordinate Co^{II} ions together with six-coordinate Co^{II} centers displaying spin-orbit coupling. In this model, the exchange interactions between the metal centers are also included. The results from both approaches are in remarkable agreement.

Results and Discussion

Synthesis: The Schiff-base ligand Hbpp is readily prepared quantitatively from the reaction of 2,6-diformyl-4-methylphenol with two equivalents of aniline (see Scheme S1 in the Supporting Information), as described in the literature.^[15] The reaction of Hbpp with an equimolar amount of Co(ClO₄)₂ in the presence of a strong base (NaOMe or NaOH) in MeOH or DMF leads to either a precipitate or crystals of **1**, respectively, following CO₂ uptake from the atmosphere, according to Equation (1).



Interestingly, the use of a weaker base, such as NEt₃ does not facilitate the trapping of CO₂ and consequently, the reaction does not proceed. On the other hand, CO₃^{2–} may be added in the form of a metallic salt to the reaction mixture, which also leads to the generation of complex **1**. Thus, addition of Co(ClO₄)₂ to a stirred methanol solution of Hbpp and K₂CO₃ leads to precipitation of the pentanuclear aggregate, as described in Equation (2).



Interestingly, the yield of both processes was very similar, even if the latter was carried out in both, aerobic and anaerobic conditions. This shows that the formation of **1** constitutes a significant driving force to the capture of CO₂ from the atmosphere if the basic conditions, necessary in this process, are met. On the other hand, no evidence of the formation of any cobalt(III) byproduct was observed. The identity of complex **1** was consistent with the results from elemental analysis. The complex was characterized spectroscopically, both by UV/Vis and IR measurements (see Experimental Section and Figure S1 and S2 in the Supporting Information). In particular, IR stretching bands characteristic of coordinated carbonate are observed at 1552 and 1381 cm^{–1}, whereas a typical imine signal occurs at 1609 cm^{–1}. The details of the molecular structure of this cluster were obtained from single-crystal X-ray diffraction experiments (see below).

Description of the structure: The molecular structure of **1** is represented in Figure 1, and crystallographic data and selected metric parameters are listed in Tables 1 and 2. This compound consists of a cationic [Co₅(CO₃)₂(bpp)₅]⁺ complex and a ClO₄[–] counterion. The cation features five Co^{II} ions disposed in a planar quasi-ideal pentagonal arrangement, and connected pairwise by the phenolate donors of five bpp[–] ligands. These five bridging oxygen atoms are located at the apices of another pentagon, approximately circumscribed around an ideal circle in which the metallic pentagon would be inscribed. Besides linking two metals through the phenolate, each bpp[–] ligand forms an additional bond to both of these metal centers through its N donor atoms. The ensemble can thus be described as a cyclic arrangement of five *fused* [Co₂(bpp)] moieties. To fit around this pentagonal topology, the ligands are bent and stacked on top of each other, mutually shifted by angles of about 70°, conforming the five blades of an imaginary propeller. This arrangement is favored by the establishment of intramolecular π···π interactions involving each phenyl ring and the phenolate cycle of the bpp moiety adjacent to it. Thus, each phenolate ring in fact forms one such interaction with two phenyl rings, one on each side. The average inclination

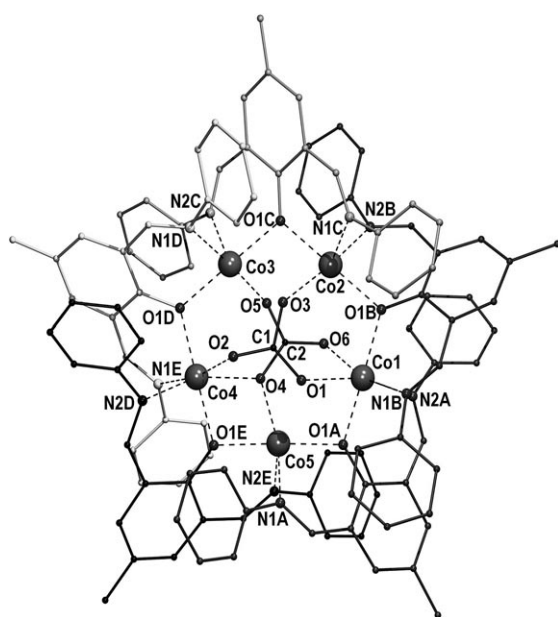


Figure 1. PovRay representation of the cation of **1**, $[\text{Co}_5(\text{CO}_3)_2(\text{bpp})_5]^+$. Hydrogen atoms are not shown for clarity. Only non-carbon atoms and CO_3^{2-} ligands are labeled. For clarity, the various bpp[−] ligands are represented in different gray scales.

of the bpp[−] phenolate rings with respect to the idealized

Table 1. Crystallographic data of complex $[\text{Co}_5(\text{CO}_3)_2(\text{bpp})_5]\text{ClO}_4\cdot\text{DMF}$ (**1**·DMF).

formula	$\text{C}_{107}\text{H}_{85}\text{Co}_5\text{N}_{10}\text{O}_{11}\cdot\text{ClO}_4\cdot\text{C}_3\text{H}_7\text{NO}$
<i>M</i>	2154.05
space group	$P2_1/n$
crystal system	monoclinic
<i>a</i> [Å]	16.5226(4)
<i>b</i> [Å]	32.6191(9)
<i>c</i> [Å]	19.3264(7)
β [°]	111.386(1)
<i>V</i> [Å ³]	9698.8(5)
<i>Z</i>	4
<i>T</i> [K]	120
ρ_{calc} [g cm ^{−3}]	1.475
<i>F</i> (000)	4436
$\mu(\text{MoK}\alpha)$ [cm ^{−1}]	9.40
measured reflections	51 015
unique reflections	13 050
<i>R</i> _{int}	0.1318
obs. refl. ns [<i>I</i> ≥ 2σ(<i>I</i>)]	7097
$\theta_{\text{min}}-\theta_{\text{max}}$ [°]	1.87–23.00
<i>hkl</i> ranges	−18,18; −35,35; −20,21
<i>R</i> (<i>F</i> ²) (observed reflections)	0.0874
<i>wR</i> (<i>F</i> ²) (all reflections)	0.2212
no. variables	1283
goodness of fit	1.024
$\Delta\rho_{\text{max}}; \Delta\rho_{\text{min}}$ [e Å ^{−3}]	1.25; −0.67

metallic polygon is 37.7°. The approximate point symmetry of this assembly is thus *D*₅. This symmetry is broken by the presence of two central CO_3^{2-} ligands, capping each face of the pentagon and mutually disposed in an approximately staggered conformation with a C⋯C distance of 2.697(2) Å.

These CO_3^{2-} molecules bind the metal centers (Figure 2) in a $\mu_{1,2,3}$ and $\mu_{1,1,2,3}$ mode, respectively ([3.111] and [3.211] in Harris notation).^[25] Such coordination modes are ascribed

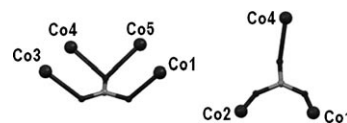


Figure 2. Mercury representation of the coordination modes of the CO_3^{2-} ligands in **1**. The Co ions involved are labeled.

on the basis of what have been considered as bonding O–Co interactions between the metal centers and the CO_3^{2-} ligands. In this complex, these are in the range of 2.033(10) to 2.224(7) Å (see Table 2 for complete list). The metal–carbonate contacts in complex **1**, not considered as bonds, are 2.420(9) Å or longer. Therefore, the coordination geometries of the metals in this cluster are either distorted octahedral with a *cis*-N₂O₄ environment (Co1 and Co4) or distorted square pyramidal with an N₂O₃ environment and axial N atoms (Co2, Co3, and Co5). The Co–O distances to the phenoxide oxygen atoms range from 1.990(7) to 2.012(6) Å. Interestingly, the Co–O–Co angles in this [(CoO)₅] ring span a range 8.5° wide (104.29–112.76°), whereas the O–Co–O angles are much more regular (176.31–178.58°). On the other hand, the Co–N lengths span from 2.136(9) to 2.214(6) Å. Within the Co pentagon, the distances between adjacent metal centers are 3.148(2) to 3.310(2) Å, and the second neighbor separations are in the range 5.165(2) to 5.252(2) Å. The crystal packing in complex **1** does not feature any obvious hydrogen bonding or π–π stacking interaction network (see Figure S3 in the Supporting Information).

Regular pentagonal arrangements of 3d metals as seen in complex **1** are virtually nonexistent, at least, with the [–(M–O)₅–] sequence. By contrast, the related hexagonal version is more common, and several examples involving CO_3^{2-} encapsulation have been reported, especially with Ni^{II}.^[26–28] On the other hand, other molecular pentagonal arrangements involving more extended bridges between metals have been reported.^[3]

Magnetic properties: The synthesis of complex **1** represents an excellent opportunity for studying the nature of the magnetic exchange within polynuclear complexes of high-spin Co^{II} ions subject to spin-orbit coupling and for probing new methodologies that are being developed to face this challenge.

DFT study of the magnetic exchange: Theoretical methods based on density functional theory have been extensively used for some time now to study the spin state of systems ranging from simple molecules^[29,30] to polynuclear metal clusters.^[31] Such methodology also allows one to determine all the exchange coupling constants present in polynuclear transition-metal complexes^[32–35] and it has been employed

here to obtain an estimate of the magnetic interactions within complex **1**. The results from this study have been useful for the phenomenological simulation of the experimental magnetization data (see below) and were rationalized in light of the structural features of the system. Originally, these calculations were attempted by employing the B3LYP functional^[36] based on all electron Gaussian basis sets. This method however, often faces insurmountable difficulties when dealing with Co^{II} ions that exhibit strong spin-orbit coupling, and this was the case in the current system (see Experimental Section). Nevertheless, the energies of the various possible spin distributions in **1** could be determined by employing the program SIESTA^[37] through a GGA exchange-correlation functional,^[38] involving only external electrons while substituting the atom cores by appropriate pseudopotentials (see Experimental Section). This method does not consider spin-orbit coupling. Nevertheless, the information this model gives on the coupling constants is very useful and may be used as a good starting point for fitting the experimental data (see below). Given the geometry of **1**, this system requires nine different coupling constants for a description of its intramolecular magnetic exchange (see Figure 3) as represented in the Hamiltonian of Equation (3).

$$\begin{aligned} \hat{H} = & -J_1\hat{S}_1\hat{S}_3 - J_2\hat{S}_2\hat{S}_4 - J_3\hat{S}_3\hat{S}_5 - J_4\hat{S}_1\hat{S}_4 - J_5\hat{S}_1\hat{S}_5 \\ & -J_6\hat{S}_1\hat{S}_2 - J_7\hat{S}_3\hat{S}_4 - J_8\hat{S}_4\hat{S}_5 - J_9\hat{S}_2\hat{S}_3 \end{aligned} \quad (3)$$

Therefore, it is necessary to calculate the energy of at least ten spin configurations,^[33,39] chosen so that a system of nine equations and nine unknowns (the J constants) can be prepared and solved. In fact, to verify possible errors or shortcomings of the procedure, we have studied the fifteen electronic configurations that are allowed by using the broken symmetry approach. These correspond to the following spin

Table 2. Selected interatomic distances [Å] and angles [°] for complex [Co₅(CO₃)₂(bpp)₃][ClO₄·DMF] (**1**-DMF).

Distances					
Co1–O1A	1.967(7)	Co2–O1B	2.002(6)	Co3–O1C	1.990(7)
Co1–N2A	2.186(8)	Co2–N2B	2.138(9)	Co3–N2C	2.150(8)
Co1–O1B	1.994(7)	Co2–O1C	1.997(7)	Co3–O1D	1.998(7)
Co1–N1B	2.214(6)	Co2–N1C	2.150(8)	Co3–N1D	2.150(6)
Co1–O1	2.189(7)	Co2–O3	2.033(10)	Co3–O3	2.454(10)
Co1–O6	2.116(7)	Co2–O6	2.732(10)	Co3–O5	2.062(10)
Co4–O1D	1.986(7)	Co5–O1A	2.012(6)	C1–O1	1.234(11)
Co4–N2D	2.159(6)	Co5–N1A	2.154(8)	C1–O2	1.245(11)
Co4–O1E	1.983(7)	Co5–O1E	2.003(6)	C1–O3	1.273(12)
Co4–N1E	2.157(9)	Co5–N1E	2.136(9)	C2–O6	1.217(12)
Co4–O2	2.093(6)	Co5–O1	2.420(9)	C2–O5	1.251(12)
Co4–O4	2.224(7)	Co5–O4	2.187(7)	C2–O4	1.284(12)
Co1–Co2	3.288(2)	O1A–O1B	3.969(10)	Co1–O1D	6.009(6)
Co1–Co5	3.214(2)	O1B–O1C	3.997(9)	Co2–O1E	6.211(7)
Co2–Co3	3.155(2)	O1C–O1D	3.979(10)	Co3–O1A	6.131(6)
Co3–Co4	3.310(2)	O1D–O1E	3.967(10)	Co4–O1B	6.058(7)
Co4–Co5	3.148(2)	O1E–O1A	4.014(8)	Co5–O1C	6.211(9)
Angles					
O1A–Co1–2A	84.9(3)	O1B–Co2–N2B	84.7(3)	O1C–Co3–N2C	84.5(3)
O1A–Co1–1B	177.9(3)	O1B–Co2–O1C	176.3(3)	O1C–Co3–O1D	177.9(3)
O1A–Co1–1B	95.8(3)	O1B–Co2–N1C	96.2(3)	O1C–Co3–N1D	94.4(3)
O1A–Co1–O1	77.1(3)	O1B–Co2–O3	102.0(3)	O1C–Co3–O3	70.4(3)
O1A–Co1–O6	99.6(3)	O1B–Co2–O6	66.6(3)	O1C–Co3–O5	88.0(4)
N2A–Co1–1B	97.0(3)	N2B–Co2–O1C	92.9(3)	N2C–Co3–O1D	97.4(3)
N2A–Co1–1B	91.9(3)	N2B–Co2–N1C	91.4(3)	N2C–Co3–N1D	88.9(3)
N2A–Co1–O1	161.0(3)	N2B–Co2–O3	167.9(4)	N2C–Co3–O3	154.1(3)
N2A–Co1–O6	94.5(3)	N2B–Co2–O6	94.3(4)	N2C–Co3–O5	95.6(4)
O1B–Co1–1B	83.5(3)	O1C–Co2–N1C	86.6(4)	O1D–Co3–N1D	84.6(3)
O1B–Co1–O1	101.0(3)	O1C–Co2–O3	80.0(4)	O1D–Co3–O3	107.9(3)
O1B–Co1–O6	81.0(3)	O1C–Co2–O6	110.9(4)	O1D–Co3–O5	92.8(4)
N1B–Co1–O1	95.9(3)	N1C–Co2–O3	97.8(4)	N1D–Co3–O3	98.8(3)
N1B–Co1–O6	163.8(3)	N1C–Co2–O6	161.2(4)	N1D–Co3–O5	175.0(4)
O1–Co1–O6	82.7(3)	O3–Co2–O6	73.4(4)	O3–Co3–O5	77.9(4)
O1D–Co4–2D	85.1(3)	O1A–Co5–N1A	85.2(3)	Co4–O4–Co5	91.1(3)
O1D–Co4–1E	178.6(3)	O1A–Co5–O1E	176.8(3)	Co1–O1A–Co5	107.4(3)
O1D–Co4–1E	96.6(3)	O1A–Co4–N2E	95.7(3)	Co1–O1B–Co2	110.7(3)
O1D–Co4–O2	84.8(3)	O1A–Co5–O1	71.2(3)	Co2–O1C–Co3	104.6(3)
O1D–Co4–O4	103.8(3)	O1A–Co5–O4	107.4(3)	Co3–O1D–Co4	112.8(3)
N2D–Co4–1E	94.2(3)	N1A–Co5–O1E	91.6(3)	Co4–O1E–Co5	104.3(3)
N2D–Co4–1E	90.4(3)	N1A–Co5–N2E	91.2(3)	Co1–O1–C1	126.4(7)
N2D–Co4–O2	169.8(3)	N1A–Co5–O4	162.8(3)	Co1–O5–C2	127.9(7)
N2D–Co4–O4	98.6(3)	N1A–Co5–O1	97.1(3)	Co2–O3–C1	132.2(8)
O1E–Co4–1E	84.6(3)	O1E–Co5–N2E	84.6(3)	Co3–O5–C2	129.3(8)
O1E–Co4–O2	95.9(3)	O1E–Co5–O1	108.9(3)	Co4–O2–C1	124.5(7)
O1E–Co4–O4	75.1(3)	O1E–Co5–O4	75.6(3)	Co4–O4–C2	122.7(7)
N1E–Co4–O2	92.2(3)	N2E–Co5–O4	98.8(3)	Co5–O4–C2	121.9(7)
N1E–Co4–O4	158.3(4)	N2E–Co5–O1	163.8(3)		
O2–Co4–O4	82.5(3)	O1–Co5–O4	76.8(3)		

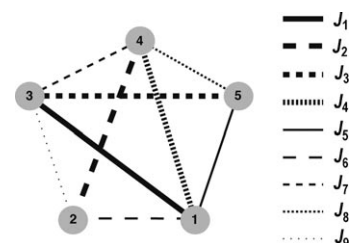


Figure 3. Representation of the spin-coupling scheme used for the DFT calculations and for modeling the magnetic data of **1**. The metal numbering is the same as used for the crystallographic description.

Table 3. Magnetic exchange coupling (J_i), bridging ligands (L), selected structural parameters (in Å and in °), metal coordination number (CN), and theoretical and experimental magnetic coupling constants (in cm^{-1}) for **1**.

J_i	Sites [i,j]	dCo-Co [Å] ^[a]	L	d(Co)-O [Å] ^[a]	d(Co ₂)-O [Å] ^[a]	Co-O-Co [°]	Co-O-C [°]	CN	J_{PBE} ^[b]	J_{exp} ^[c]
J_1	[1, 3]	5.195	$\mu\text{-CO}_3$	2.116	2.062	—	127.9(7) 129.3(8)	6, 5	−5.9(5)	−3.5
J_2	[2, 4]	5.222	$\mu\text{-CO}_3$	2.032	2.093	—	132.2(8) 124.5(7)	5, 6	−4.9(5)	−3.5
J_3	[3, 5]	5.222	$\mu\text{-CO}_3$	2.062	2.187	—	129.3(8) 121.9(7)	5, 5	−3.2(5)	−3.5
J_4	[1, 4]	5.165	$\mu\text{-CO}_3$	2.116	2.224	—	126.4(7)	6, 6	−1.5(5)	−0.3
			$\mu\text{-CO}_3$	2.189	2.093	—	124.5(7)			
						—	127.9(7) 122.7(7)			
J_5	[1, 5]	3.214	$\mu\text{-CO}_3$	2.116	2.187	—	—	6, 5	+0.5(5)	+0.3
			$\mu\text{-OPh}$	1.977	2.012	107.3	—			
J_6	[1, 2]	3.288	$\mu\text{-CO}_3$	2.189	2.032	—	—	6, 5	−1.1(5)	−0.3
			$\mu\text{-OPh}$	1.994	2.003	110.7	—			
J_7	[3, 4]	3.310	$\mu\text{-CO}_3$	2.062	2.224	—	—	5, 6	−6.0(5)	−3.5
			$\mu\text{-OPh}$	1.988	1.986	112.8	—			
J_8	[4, 5]	3.148	$\mu\text{-OCO}_2$	2.224	2.187	91.0	—	6, 5	−0.4(5)	−0.3
			$\mu\text{-OPh}$	1.983	2.004	104.3	—			
J_9	[2, 3]	3.155	$\mu\text{-OPh}$	1.997	1.991	104.6	—	5, 5	−0.9(5)	−0.3

[a] Labels 'i' and 'f' are used to specify the initial and final metal atom in the magnetic coupling. [b] Coupling constants obtained from DFT calculations. [c] Coupling constants obtained from fitting the experimental data.

states (only spin down centers indicated, using the notation of Figure 3): one $S=15/2$, five $S=9/2$ ([1], [2], [3], [4] and [5]) and ten $S=3/2$ ([1, 2], [1, 3], [1, 4], [1, 5], [2, 3], [2, 4], [2, 5], [3, 4], [3, 5] and [4, 5]). The values of the nine J_i constants resulting from these calculations are given in Table 3 (see Figure 3 for notation). These results allow one to draw the following conclusions: i) Regardless of the coordination number of the metals, all the pathways involving only one carbonate ligand (J_1 , J_2 , J_3) lead to similar J values of strength seemingly correlated to the average Co-O-C angles; ii) despite being mediated by two CO_3^{2-} bridges, the coupling J_4 is weaker than these above, presumably because it occurs through longer Co-O bonds and narrower Co-O-C angles (on average); iii) the pathways leading to J_5 , J_6 , and J_7 are one *syn,syn*- CO_3^{2-} and one phenoxo-like bridge. This combination is expected to lead to a ligand counter-complementarity effect on the coupling strength,^[40,41] by which, the interaction of each type of ligand with the metallic magnetic orbitals causes a decrease of the energy gaps between SOMOs, thereby diminishing the strength of the antiferromagnetic (AF) coupling. As observed before,^[40,41] this also causes a shift towards larger values of the M-O-M angle at which the interaction switches from ferromagnetic (F) to AF in phenoxo-bridged systems (θ_{SWITCH}). The calculations on **1** indicate that this switch occurs now towards 109°; iv) for the case of J_8 , the metals exhibit two monoatomic $\mu\text{-O}$ bridges, thus precluding the effect of counter-complementarity. As it turns out, the average Co-O-Co angle featured in this moiety (97.7°) is close to θ_{SWITCH} for bis-($\mu\text{-hydroxo}$)-copper(II) complexes. A similar θ_{SWITCH} might be expected here since the magnetic orbital that most efficiently propagates the exchange ($d_{x^2-y^2}$) is the same as with copper. Therefore, a very weak coupling should be observed. In agreement with the calculated value; v) the constant J_9 is expected to be AF and weaker than J_8 because there is only one $\mu\text{-O}$ bridge. It is however slightly more negative than J_8

because the Co-O-Co angle (104.6°) is wider and therefore, further within the space corresponding to AF coupling.

Bulk magnetization measurements: Variable-temperature magnetization measurements were performed on a powdered polycrystalline sample of **1** under a constant magnetic field of 0.5 T, in the 2–300 K range. The results are represented in Figure 4 as $\chi_M T$ versus T plots (χ_M being the molar

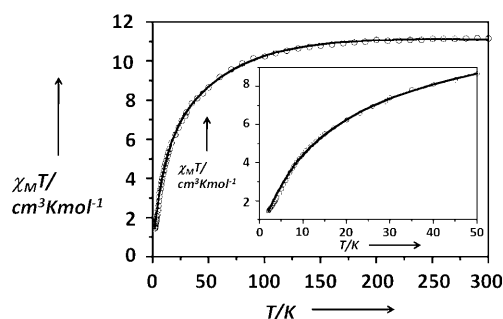


Figure 4. Plots of $\chi_M T$ versus T per mole of $[\text{Co}_5(\text{CO}_3)_2(\text{bpp})_5]\text{ClO}_4$ (**1**). The solid lines are the fit of the experimental data through a matrix diagonalization technique (see text).

paramagnetic susceptibility of the compound). At room temperature, $\chi_M T$ is $11.16 \text{ cm}^3 \text{ K mol}^{-1}$, significantly larger than expected for five magnetically isolated high-spin Co^{II} ions ($\chi_M T = 9.375 \text{ cm}^3 \text{ K mol}^{-1}$ if $g=2$), which indicates that the orbital angular momentum of the metal ions is not quenched and therefore contributes significantly to χ_M . Upon cooling, $\chi_M T$ decreases at an increasingly faster rate, reaching a value of $1.52 \text{ cm}^3 \text{ K mol}^{-1}$ at 2 K, where the curve seems to initiate a tendency to level off. This decline, which leads to values much lower than could be expected for five non-interacting high-spin Co^{II} ions exhibiting spin-orbit cou-

pling, clearly indicates the presence of AF coupling between the metal centers, consistent with the results obtained from DFT calculations (see above). The strong orbital contribution to the magnetic moment precludes the possibility of using the spin-only formalism as a model to simulate the experimental data, thus rendering this problem extremely complex. Some of us have developed procedures to interpret the magnetic behavior of polynuclear Co^{II} clusters, taking into account the effects of spin-orbit coupling.^[14] Complex **1** constitutes a good object of study to verify the validity of these methods (see below).

Simulation of the magnetic data: A matrix diagonalization method including spin-orbit coupling effects, based on a perturbational approach, has been recently proposed by some of us as a tool to describe the magnetic properties of six-coordinate high-spin Co^{II} clusters.^[14] This method is used here to describe the magnetic behavior of **1**. Since the details are published elsewhere, only a summary is provided below.

It is known that in a purely octahedral symmetry, the ground term ⁴F of a high-spin Co^{II} ion is split into three states, ⁴T_{1g}, ⁴T_{2g}, and ⁴A_{2g}, of which the former is the ground state and is well separated (more than 8000 cm⁻¹) from the other two. In addition, first-order spin-orbit coupling splits the ⁴T_{1g} ground state into a sextet, a quadruplet, and a Kramer's doublet, the eigenfunctions of which can be obtained by diagonalization of the matrix obtained from the Hamiltonian in Equation (4).

$$\hat{H} = -A\kappa\lambda\hat{L}\hat{S} \quad (4)$$

In this Hamiltonian, κ and A are orbital reduction factors associated, respectively, with the covalent character of the metal-ligand bonds and with the interaction of the ⁴T_{1g} state (⁴T_{1g}[F]) with an excited ⁴T_{1g} state from a P term (⁴T_{1g}[P]). Typical values of κ lie within the range of 0.75 to 1, whereas A , which provides a measure of the ligand field strength, takes values between 3/2 (weak field limit) and 1 (strong field limit). The parameter λ is the spin-orbit constant that, because of the covalence of the metal-ligand bond, has a lower value than expected for the free ion. Most real systems of Co^{II}, however, display distortions from the ideal octahedral geometry, which lead (for the case of an axial distortion) to a splitting of the triplet orbital state ⁴T_{1g} into two other states, ⁴A_{2g} and ⁴E_g, separated by an energy gap, Δ . Considering the consequences of this distortion and using the T and P term isomorphism, the Hamiltonian given in Equation (5) can be used to describe the system, now involving the spin-orbit coupling, the axial distortion

and the Zeeman interaction with an external magnetic field B .

$$\begin{aligned} \hat{H} = & -A\kappa\lambda\hat{L}\hat{S} + \Delta\left[\hat{L}_z^2 - 1/3L(L+1)\right] \\ & + \mu_B\left[-A\kappa\hat{L} + g_e\hat{S}\right]B \end{aligned} \quad (5)$$

This Hamiltonian does not provide for an analytical expression of χ_M as a function of the parameters A , κ , λ and Δ , thus, their values must be determined through a numerical matrix diagonalization method. This may be done by making the analogy of this Hamiltonian with that for a hypothetical system composed of two local exchange-coupled spin moments ($L=1$ and $S=3/2$) and very different g values of $A\kappa$ and g_e , respectively. The spin triplet (represented by L) would be seen as experiencing axial zero field splitting (ZFS) quantified by Δ with the coupling between both centers being gauged by $A\kappa\lambda$. Under this analogy, represented in Figure 5A, the first term of Equation (5) is the spin-spin coupling, the second term is the energy of the ZFS, and the third represents the Zeeman splitting of both local spins. This procedure would allow one to obtain the temperature dependence of χ_M for a mononuclear cobalt(II) complex. Nevertheless, it can be expanded to include more metal ions and the coupling between them.^[42,43] Complex **1** exhibits five nonequivalent Co^{II} ions, which could, for simplicity, be treated using average values of the spin-orbit coupling parameters. However, the system contains metals with coordination numbers five and six. The former centers must exhibit very large values of Δ and may thus be treated as quartets ($S=3/2$) subject to ZFS (thus, as in the spin-only formalism). In fact, attempts to treat the problem as five equivalent metal centers only resulted in unreasonable average values for the various parameters. By contrast, considering three anisotropic $S=3/2$ centers together with two Co^{II} ions with strong spin-orbit coupling, thus involving L and S , (Figure 5B) resulted in the successful simulation of the experimental data. Under this approach, the lowest possible value expected for $\chi_M T$ (8.9 cm³ K mol⁻¹ at 0 K, for three $S=3/2$ spin-only centers with $g=2$ and two octahedral Co^{II} ions with only the

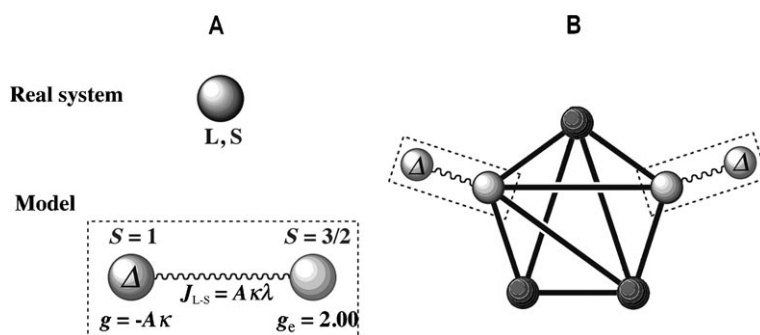


Figure 5. A) Representation of the model employed for a high-spin six-coordinate Co^{II} system with spin-orbit coupling. It is modeled as two local spins, $S=1$ (subject to a ZFS, Δ) and $S=3/2$ with g values of $g = -A\kappa$ and g_e , respectively, and coupled (with a coupling constant $A\kappa\lambda$). B) Application of the model to a cluster incorporating two six-coordinate Co^{II} ions with spin-orbit coupling and three five-coordinate Co^{II} metals (darker balls, treated as spin-only centers with $S=3/2$).

lowest Kramer doublet populated, all uncoupled) is much higher than observed experimentally for a wide range of temperatures (see Figure 4), which clearly indicates the presence of AF interactions within the complex. As mentioned before, the coupling between Co^{II} centers may be treated with the model proposed here. Assuming that the exchange coupling only contains isotropic contributions operating on the real spins of the Co^{II} ions, the coupling scheme in Figure 3 may be considered, where J_i represent constants for the interactions between $S=3/2$ spins. Even including all the approximations described above, the diagonalization of the resulting matrix (with the parameters A , κ , λ , Δ and J_i) continues to be prohibitive. However, if J is smaller than λ (i.e. $J/\lambda < 0.1$), as is usually the case, a perturbative approach can be implemented, thereby simplifying dramatically the problem. Under these conditions, each of the Co^{II} ions with spin-orbit coupling may be considered as just an effective local spin moment with $S_{\text{eff}}=1/2$, exhibiting a g factor that depends, not only on A , κ , λ , and Δ , but also on the temperature (termed $G(T)$). The coupling constants between the so defined local spins become now *effective* coupling constants (J') and their relation with the corresponding real constants is $J'=25J/9$ (coupling between two $S_{\text{eff}}=1/2$) or $J'=5J/3$ (coupling between a $S_{\text{eff}}=1/2$ and a $S=3/2$).^[14] The value of $G(T)$ at each temperature may be obtained either by using a reported empirical law or by matrix diagonalization.^[14] The latter method is used here, since it is more exact. The description of the magnetic exchange in complex **1** requires nine coupling constants (Figure 3). To avoid overparameterization, which causes the presence of several local error minima, the various J parameters have been grouped into three categories (J_a [J_1, J_2, J_3, J_7]; J_b [J_4, J_6, J_8, J_9]; J_c [J_5]) using the information obtained from DFT calculations. Using this procedure, good simulations of the experimental data were obtained, by using the program VPMAG,^[44] for several sets of parameters. Some of these however, lacked any reasonable physical meaning and only solutions involving moderate to strong metal–ligand covalence, as expected for this system, were considered. The best fit (see Figure 3) was obtained for the following parameters; i) $A\kappa=1.06$, $\lambda=-126\text{ cm}^{-1}$, $\Delta=+1.1\text{ cm}^{-1}$ (six-coordinate Co^{II} ions), ii) $g=2.049$ and $D=+0.7\text{ cm}^{-1}$ (five-coordinate, $S=3/2$ Co^{II} ions), and iii) $J_a=-3.5\text{ cm}^{-1}$, $J_b=-0.3\text{ cm}^{-1}$ and $J_c=+0.3\text{ cm}^{-1}$. The small value of Δ resulting from this fit is consistent with the high symmetry of the six-coordinate Co^{II} centers present in **1**. In addition, the g and D parameters associated with the five-coordinate ions fall perfectly within the expected ranges.^[45] Finally, the good agreement between the experimental data and the curve arising from this fit must be highlighted, as well as the consistency between the coupling constants obtained here and the values arising from DFT calculations. These factors serve to validate the approach and approximations used during this study, which demonstrates that the method employed serves to obtain physically meaningful values for various important parameters governing the magnetic behavior of high-spin Co^{II} clusters.

Conclusions

The particular geometric features of the $[\text{Co}^{\text{II}}_2(\text{bpp})]$ moiety facilitates the capture of atmospheric CO_2 (in the form of carbonate ligands) and the assembly of a peculiar pentagonal architecture with the shape of a propeller. This symmetry forces the CO_3^{2-} ligands to lie in irregular coordination modes (unlike what is observed when carbonate templates the formation of more common cyclic hexagonal arrangements), yielding a combination of five- and six-coordinate high-spin Co^{II} ions. Modeling the magnetic properties of such molecules is highly challenging, and the title system has served as a good test for the validity of a matrix diagonalization technique, recently developed to treat polynuclear molecules of Co^{II} . The validity of the method is corroborated by both the success in reproducing the experimental data and the agreement with the results obtained from DFT calculations on this $[\text{Co}^{\text{II}}_5]$ cluster.

Experimental Section

Synthesis: The chemicals used were obtained from the following sources: *p*-cresol, *para*-formaldehyde, hexamine, and aniline from SRL Chem (India) and sodium methoxide from Spectrochem (India). Cobalt perchlorate hexahydrate was prepared by treating cobalt(II) carbonate with HClO_4 (1:1) and crystallized after concentration on a water bath. 2,6-Bis(phenyliminomethyl)-4-methylphenolate (Hbpp) was prepared by a literature procedure.^[15] All other chemicals and solvents were reagent grade materials and were used as received without further purification. All the reactions were performed in air at room temperature, unless otherwise indicated.

$[\text{Co}_2(\text{CO}_3)_2(\text{bpp})_2]\text{ClO}_4\cdot\text{DMF}$ (1-DMF): Method 1: To an orange solution of Hbpp (0.31 g, 1 mmol) in MeOH (25 mL) was added dropwise a solution of $\text{Co}(\text{ClO}_4)_2\cdot 6\text{H}_2\text{O}$ (0.73 g, 2 mmol) in MeOH (25 mL) with stirring, followed by addition of solid NaOMe (0.22 g, 4 mmol). The stirring was maintained for 3 h. A mustard-brown precipitate was collected by filtration, washed with cold methanol and water, and dried under vacuum over P_4O_{10} . The yield of **1** was 74 %. Single crystals of the complex, suitable for X-ray analysis were obtained from DMF, by dissolving **1** (250 mg) in this solvent (10 mL) and leaving the resulting solution unperturbed and open to the atmosphere for five days. Elemental analysis calcd (%) for $\text{C}_{110}\text{H}_{92}\text{N}_{10}\text{O}_{16}\text{ClCo}_5$ (2154.1): C 61.33, H 4.30, N 7.15; found: C 61.25, H 4.21, N 6.94; selected FTIR bands: (KBr): $\tilde{\nu}=3447$ (br), 1609 (s), 1590 (s), 1552 (vs), 1488 (m), 1430 (s), 1381 (m), 1325 (m), 1195 (s), 1072 (s), 756 (vs), 693 (s), 534 cm^{-1} (m); molar conductance, Λ_{M} : (DMF solution): 70 $\text{ohm}^{-1}\text{cm}^2\text{mol}^{-1}$; UV/Vis spectra [λ_{max} (ε)]: (DMF solution): 400 (4665), 276 nm (12495 $\text{Lmol}^{-1}\text{cm}^{-1}$).

Method 2: K_2CO_3 (0.55 g, 4 mmol) was dissolved in degassed methanol (40 mL) by stirring for 3 h. The ligand Hbpp (0.31 g, 1 mmol) was dissolved in degassed methanol (20 mL) and the solution was added dropwise with stirring to the previous one. The resulting orange solution was stirred for about 10 min, and a solution of $\text{Co}(\text{ClO}_4)_2\cdot 6\text{H}_2\text{O}$ (0.73 g, 2 mmol) in degassed methanol (15 mL) was added to it dropwise. The reaction mixture was stirred further for 2 h. A mustard-brown precipitate of **1** was collected by filtration, washed with cold methanol followed by water, and dried under vacuum over P_4O_{10} . The yield was 72 %.

Caution! Although no problems were encountered in this study, transition metal perchlorates are potentially explosive and should be handled with care.

Single-crystal X-ray crystallography: The crystal data of compound 1-DMF were collected at 120 K using a Nonius Kappa CCD diffractometer with graphite-monochromated MoK_{α} radiation. The data sets were in-

tegrated with the Denzo-SMN package^[46] and corrected for Lorentz, polarization and absorption effects (SORTAV).^[47] The structure was solved by direct methods (SIR97)^[48] and refined by using full-matrix least-squares with all non-hydrogen atoms anisotropically and hydrogens included at calculated positions, riding on their carrier atoms. The asymmetric unit is built up by a pentanuclear cation complex $[(\text{Co bpp})_5(\text{CO}_3)_2]^+$, a ClO_4^- ion, and a DMF solvent molecule. All calculations were performed by using SHELXL-97^[49] and PARST^[50] implemented in the WINGX^[51] system of programs. The crystal data are given in Table 1. Selected bond lengths and angles are given in Table 2. CCDC-736764 contains the supplementary crystallographic data for this paper. These data can be obtained free of charge from The Cambridge Crystallographic Data Centre via www.ccdc.cam.ac.uk/data_request/cif.

Physical measurements: Microanalyses were performed by using a Perkin-Elmer model 2400 microanalyzer. FT-IR spectra were recorded on a Perkin-Elmer RX1 spectrometer. The solution electrical conductivity and electronic spectra were obtained by using a Unitech type U131C digital conductivity meter with a solute concentration of about 10^{-3} M and a Shimadzu 1601 UV-Vis-NIR spectrophotometer, respectively. ^1H and ^{13}C NMR spectra were recorded in CDCl_3 with a Bruker AC 200 NMR Spectrometer using TMS as the internal standard. Variable-temperature magnetic susceptibility data were obtained with a Quantum Design MPMS5 SQUID magnetometer. The field applied for temperature-dependent measurements was in the range of linear dependence of M versus H . The measured values were corrected for the experimentally determined contribution of the sample holder, while Pascal's constants were utilized to estimate diamagnetic corrections to the molar paramagnetic susceptibility.

Computational details: Calculations were performed through the Gaussian09 package using the B3LYP functional,^[36] the quadratic convergence approach and a guess function generated with the Jaguar 6.5 code.^[52] The usual procedure involving triple- ζ and double- ζ all-electron Gaussian basis sets for the metal and the rest of atoms, respectively, gave no satisfactory results.^[53,54] Calculations engaging 4 Itanium2 1.3 GHz processors either did not meet the convergence criterion after eight weeks, as a result of fluctuations in the process, or led to an extremely slow convergence when using a quadratic convergence algorithm. This is common with systems containing cobalt(II) ions with strong spin-orbit coupling. Spin distributions have been calculated by employing the program SIESTA (Spanish Initiative for Electronic Simulations with Thousands of Atoms).^[30] As done previously, the GGA exchange-correlation functional proposed by Perdew, Burke, and Ernzerhof (PBE) was used here.^[38] Only external electrons are included in the calculations, the cores being replaced by norm-conserving scalar relativistic pseudopotentials factorized in the Kleinman-Bylander form.^[55] These pseudopotentials are generated following the approach proposed by Trouiller and Martins^[56] from the ground state atomic configurations for all the atoms except for Co, for which, the configuration $[\text{Ne}]3s^23p^64s^03d^7$ was employed. The core radii for the s, p, d, and f components of the Co atoms are 2.38, 2.44, 2.26, and 2.26, respectively.^[57] The cutoff radii were 1.14 for oxygen, nitrogen, and hydrogen atoms and 1.25 for carbon atoms, respectively. Similar problems observed with Gaussian packages were also found here. A search for the optimum parameters for the energy shift and for the mesh cutoff allowed us, after considerable efforts, to obtain good converged electronic configurations.

Acknowledgements

M.S. acknowledges the CSIR, New Delhi, India for her doctoral fellowship. V.B. acknowledges Italian Ministry of University and Scientific Research (MIUR, Rome). G.A. and J.C. acknowledge the Spanish Ministry of Science and Education (Projects CTQ2007-61690, CTQ2009-06959 and CSD2007-00010). G.A. thanks the Generalitat de Catalunya for the prize ICREA Academia 2008. J.C. thanks the Generalitat Valenciana (Program PROMETEO/2009/108). The authors thankfully acknowledge the computer resources, technical expertise, and assistance provided by the

Red Española de Supercomputación (RES), by the Barcelona Supercomputing Center (BCS), and by the Supercomputing Center of the Universitat de València (Tirant).

- [1] D. Mandal, V. Bertolasi, G. Aromí, D. Ray, *Dalton Trans.* **2007**, 1989–1992.
- [2] C. L. Chen, J. Y. Zhang, C. Y. Su, *Eur. J. Inorg. Chem.* **2007**, 2997–3010.
- [3] C. S. Campos-Fernández, B. L. Schottel, H. T. Chifotides, J. K. Bera, J. Bacsá, J. M. Koomen, D. H. Russell, K. R. Dunbar, *J. Am. Chem. Soc.* **2005**, *127*, 12909–12923.
- [4] R. Sessoli, D. Gatteschi, A. Caneschi, M. A. Novak, *Nature* **1993**, *365*, 141–143.
- [5] G. Aromí, E. K. Brechin, *Struct. Bonding* **2006**, *122*, 1–67.
- [6] A. L. Barra, L. C. Brunel, D. Gatteschi, L. Pardi, R. Sessoli, *Acc. Chem. Res.* **1998**, *31*, 460–466.
- [7] L. Lecren, W. Wernsdorfer, Y. G. Li, O. Roubeau, H. Miyasaka, R. Clerac, *J. Am. Chem. Soc.* **2005**, *127*, 11311–11317.
- [8] M. Murrie, *Chem. Soc. Rev.* **2010**, *39*, 1986–1995.
- [9] Y. Z. Zheng, M. L. Tong, W. X. Zhang, X. M. Chen, *Angew. Chem.* **2006**, *118*, 6458–6462; *Angew. Chem. Int. Ed.* **2006**, *45*, 6310–6314.
- [10] M. E. Lines, *J. Chem. Phys.* **1971**, *55*, 2977–2984.
- [11] A. V. Pali, B. S. Tsukerblat, E. Coronado, J. M. Clemente-Juan, J. J. Borrás-Almenar, *Inorg. Chem.* **2003**, *42*, 2455–2458.
- [12] H. Sakiyama, R. Ito, H. Kumagai, K. Inoue, M. Sakamoto, Y. Nishida, M. Yamasaki, *Eur. J. Inorg. Chem.* **2001**, 2027–2032.
- [13] S. M. Ostrovsky, K. Falk, J. Pelikan, D. A. Brown, Z. Tomkowicz, W. Haase, *Inorg. Chem.* **2006**, *45*, 688–694.
- [14] F. Lloret, M. Julve, J. Cano, R. Ruiz-García, E. Pardo, *Inorg. Chim. Acta* **2008**, *361*, 3432–3445.
- [15] J. J. Grzybowski, F. L. Urbach, *Inorg. Chem.* **1980**, *19*, 2604–2608.
- [16] W. J. Gu, Y. Z. Li, Y. Pan, S. H. Liu, *Acta Crystallogr. Sect. E.* **2005**, *61*, m614–m615.
- [17] L. Q. Han, W. H. Sun, L. Y. Wang, H. G. Wang, Y. Cui, *J. Chem. Crystallogr.* **2003**, *33*, 159–163.
- [18] D. Luneau, J. M. Savariault, J. P. Tuchagues, *Inorg. Chem.* **1988**, *27*, 3912–3918.
- [19] G. J. T. Cooper, G. N. Newton, D. L. Long, P. Kogerler, M. H. Rosnes, M. Keller, L. Cronin, *Inorg. Chem.* **2009**, *48*, 1097–1104.
- [20] R. P. Doyle, P. E. Kruger, B. Moubaraki, K. S. Murray, M. Nieuwenhuyzen, *Dalton Trans.* **2003**, 4230–4237.
- [21] M. Fondo, A. M. García-Deibe, M. Corbella, E. Ruiz, J. Tercero, J. Sanmartín, M. R. Bermejo, *Inorg. Chem.* **2005**, *44*, 5011–5020.
- [22] E. García-España, P. Gavina, J. Latorre, C. Soriano, B. A. Verdejo, *J. Am. Chem. Soc.* **2004**, *126*, 5082–5083.
- [23] P. Mukherjee, M. G. B. Drew, M. Estrader, A. Ghosh, *Inorg. Chem.* **2008**, *47*, 7784–7791.
- [24] C. Pariya, V. G. Puranik, N. R. Chaudhuri, *Chem. Commun.* **1997**, 1307–1308.
- [25] R. A. Coxall, S. G. Harris, D. K. Henderson, S. Parsons, P. A. Tasker, R. E. P. Winpenny, *J. Chem. Soc. Dalton Trans.* **2000**, 2349.
- [26] M. L. Tong, M. Monfort, J. M. C. Juan, X. M. Chen, X. H. Bu, M. Ohba, S. Kitagawa, *Chem. Commun.* **2005**, 233–235.
- [27] A. Graham, S. Meier, S. Parsons, R. E. P. Winpenny, *Chem. Commun.* **2000**, 811–812.
- [28] A. N. Georgopoulou, C. P. Raptopoulou, V. Psycharis, R. Balles-teros, B. Abarca, A. K. Boudalis, *Inorg. Chem.* **2009**, *48*, 3167–3176.
- [29] A. Goursot, J. P. Malrieu, D. R. Salahub, *Theor. Chim. Acta* **1995**, *91*, 225–236.
- [30] J. M. Soler, E. Artacho, J. D. Gale, A. García, J. Junquera, P. Ordejon, D. Sánchez-Portal, *J. Phys. Condens. Matter* **2002**, *14*, 2745–2779.
- [31] M. Castro, D. R. Salahub, *Phys. Rev. B* **1993**, *47*, 10955–10958.
- [32] D. Mandal, V. Bertolasi, J. Ribas-Ariño, G. Aromí, D. Ray, *Inorg. Chem.* **2008**, *47*, 3465–3467.
- [33] E. Ruiz, P. Alemany, S. Alvarez, J. Cano, *J. Am. Chem. Soc.* **1997**, *119*, 1297–1303.

- [34] E. Ruiz, J. Cano, S. Alvarez, A. Caneschi, D. Gatteschi, *J. Am. Chem. Soc.* **2003**, *125*, 6791–6794.
- [35] E. C. Sañudo, T. Cauchy, E. Ruiz, R. H. Laye, O. Roubeau, S. J. Teat, G. Aromí, *Inorg. Chem.* **2007**, *46*, 9045–9047.
- [36] A. D. Becke, *J. Chem. Phys.* **1993**, *98*, 5648–5652.
- [37] E. Artacho, J. D. Gale, A. García, J. Junquera, R. M. Martin, P. Ordejón, D. Sánchez-Portal, J. M. Soler, *SIESTA* **2001**, 1.3.
- [38] J. P. Perdew, K. Burke, M. Ernzerhof, *Phys. Rev. Lett.* **1996**, *77*, 3865–3868.
- [39] E. Ruiz, J. Cano, S. Alvarez, P. Alemany, *J. Am. Chem. Soc.* **1998**, *120*, 11122–11129.
- [40] L. Gutierrez, G. Alzuet, J. A. Real, J. Cano, J. Borrás, A. Castineiras, *Eur. J. Inorg. Chem.* **2002**, 2094–2102.
- [41] V. McKee, M. Zvagulis, J. V. Dagdigan, M. G. Patch, C. A. Reed, *J. Am. Chem. Soc.* **1984**, *106*, 4765–4772.
- [42] G. Aromí, H. Stoeckli-Evans, S. J. Teat, J. Cano, J. Ribas, *J. Mater. Chem.* **2006**, *16*, 2635–2644.
- [43] M. Fondo, N. Ocampo, A. M. Garcia-Deibe, M. Corbella, M. S. El Fallah, J. Cano, J. Sanmartin, M. R. Bermejo, *Dalton Trans.* **2006**, 4905–4913.
- [44] J. Cano, VPMAG package University of Valencia, Valencia, **2003**.
- [45] R. Boča, *Struct. Bonding* **2006**, *117*, 1–264.
- [46] Z. Otwinowski, Z. Minor, in *Methods in Enzymology*, Vol. 276, Part A (Eds.: R. M. Sweet, C. W. Carter, J. N. Abelson, M. I. Simon), Academic Press, London, **1977**, p. 307.
- [47] R. H. Blessing, *Acta Crystallogr. Sect. A* **1995**, *51*, 33.
- [48] A. Altomare, M. C. Burla, M. Camalli, G. L. Cascarano, C. Giacovazzo, A. Guagliardi, A. G. G. Moliterni, G. Polidori, R. Spagna, *J. Appl. Crystallogr.* **1999**, *32*, 115–119.
- [49] G. M. Sheldrick, SHELXL97, Program for Crystal Structure Refinement, University of Göttingen, Göttingen, Germany, **1997**.
- [50] M. Nardelli, *J. Appl. Crystallogr.* **1995**, *28*, 659.
- [51] L. J. Farrugia, *J. Appl. Crystallogr.* **1999**, *32*, 837.
- [52] Jaguar 6.0, Schrödinger, Inc., Portland, **2005**.
- [53] A. Schäfer, H. Horn, R. Ahlrichs, *J. Chem. Phys.* **1992**, *97*, 2571–2577.
- [54] A. Schäfer, C. Huber, R. Ahlrichs, *J. Chem. Phys.* **1994**, *100*, 5829–5835.
- [55] L. Kleinman, D. M. Bylander, *Phys. Rev. Lett.* **1982**, *48*, 1425–1428.
- [56] N. Troullier, J. L. Martins, *Phys. Rev. B* **1991**, *43*, 1993–2006.
- [57] S. G. Louie, S. Froyen, M. L. Cohen, *Phys. Rev. B* **1982**, *26*, 1738–1742.

Received: May 21, 2010

Published online: October 13, 2010